Molecular Therapy
Oncolytics
Original Article

Therapeutic effects of mesenchymal stem cells loaded with oncolytic adenovirus carrying decorin on a breast cancer lung metastatic mouse model

Yuning Zhang,[1,6] Chao Liu,[1,6] Tao Wang,[2] Fanxuan Kong,[1,3] Huan Zhang,[4] Jing Yi,[1] Xiwen Dong,[1] Han Duan,[1] Ning Tao,[1] Yuefeng Yang,[5] and Hua Wang[1]

[1]Department of Experimental Haematology, Beijing Institute of Radiation Medicine, 27 Taiping Road, Beijing 100850, P.R. China; [2]Oncology Department, The Fifth Medical Center of PLA General Hospital, Beijing 100071, P.R. China; [3]PLA Strategic Support Force Characteristic Medical Center, Beijing 100101, P.R. China; [4]Department of Critical Care Medicine, Beijing Tongren Hospital, Capital Medical University, Beijing 100730, P.R. China; [5]Department of Experimental Medical Science, HwaMei Hospital, University of Chinese Academy of Sciences, Ningbo 315000, Zhejiang Province, P.R. China

Oncolytic adenoviruses (OAds) are alternative immune therapeutic strategies for tumors. However, liver uptake and antibody neutralization are two major barriers for systemic delivery during the treatment of tumor metastasis. Mesenchymal stem cells (MSCs) have emerged as potential vehicles to improve delivery. In this study, we loaded umbilical-cord-derived MSCs (UC-MSCs) with OAds expressing decorin (rAd.DCN) or without foreign genes (rAd.Null) to treat breast cancer lung metastasis. *In vivo*, rAd.Null, MSCs.Null, and rAd.DCN exhibited antitumor effects compared with other groups in a mouse model. Unexpectedly, MSCs.Null showed much greater antitumor responses than MSCs.DCN, including improved survival and reduced tumor burden. Compared with rAd.Null, both MSCs.Null and MSCs.DCN could improve the viral spread and distribution in metastatic tumor lesions in the lung. MSCs.DCN produced much more decorin in lungs than rAd.DCN; however, rAd.DCN reduced the downstream target genes of decorin much more strongly than MSCs.DCN, which was consistent with *in vitro* findings. In addition, rAd.DCN, MSCs.Null, and MSCs.DCN could reduce The cytokine levels in the lung. In conclusion, MSCs improved oncolytic adenoviral delivery and spread in tumor tissues and enhanced therapeutic effects. However, MSCs.DCN reduced OAd-evoked antitumor responses, possibly via a contact-dependent mechanism.

INTRODUCTION

Breast cancer was the most common tumor and the leading cause of cancer death among females worldwide in 2018.[1] It has been demonstrated that distal metastasis is a pivotal and fatal step in the progression of various solid malignancies, including breast cancer.[2,3] The bones and lungs are favorite target organs of breast cancer distal metastasis. Bone and lung metastatic lesions could be detected in 30%–60% and 21%–32% of the population of breast cancer patients with metastases, respectively.[4–6] Although a variety of methods are available for treating breast cancer lung metastasis, such as chemotherapy, radiotherapy, and targeted therapy, the median survival is still low, and it is estimated that approximately 60%–70% of patients who die of breast cancer have lung metastatic lesions.[7,8] Therefore, the development of a novel and more effective approach to treat breast cancer lung metastasis is an urgent need.

Decorin, a natural inhibitor of transforming growth factor β (TGF-β) signaling, can negatively target several tumor-growth- and metastasis-associated signaling pathways. For example, it can suppress Met and vascular endothelial growth factor A (VEGFA) to disrupt the angiogenic network.[9–12] Moreover, decorin can improve the antitumor microenvironment by regulating inflammatory responses.[13] In recent years, our group has focused on oncolytic adenoviral therapy for distal metastasis of breast cancer and found that the oncolytic adenovirus encoding decorin, rAd.DCN, could significantly inhibit tumor growth and metastasis by suppressing Met, VEGF, and the wnt/β-catenin signaling pathway, as well as by activating antitumor immune responses.[14,15]

Mesenchymal stem cells (MSCs) can not only home to injured tissues and repair them by secreting various bioactivators but can also be recruited to the tumor site.[16–20] Therefore, MSCs have emerged as promising vehicles for therapeutic cytokine gene delivery in cancer therapy.[19,21–23] However, some studies also indicate that MSCs can migrate toward primary tumors and metastatic sites, promoting tumor progression by inhibiting the activities of immune cells.[24,25]

Received 8 July 2021; accepted 27 January 2022;
https://doi.org/10.1016/j.omto.2022.01.007.

[6]These authors contributed equally

Correspondence: Hua Wang, MD, Department of Experimental Haematology, Beijing Institute of Radiation Medicine, 27 Taiping Road, Beijing 100850, P.R. China.
E-mail: 18511712135@163.com; wanghua@bmi.ac.cn
Correspondence: Yuefeng Yang, MD, Department of Experimental Medical Science, HwaMei Hospital, University of Chinese Academy of Sciences, Ningbo 315000, Zhejiang Province, P.R. China.
E-mail: yuefengyang1981@163.com

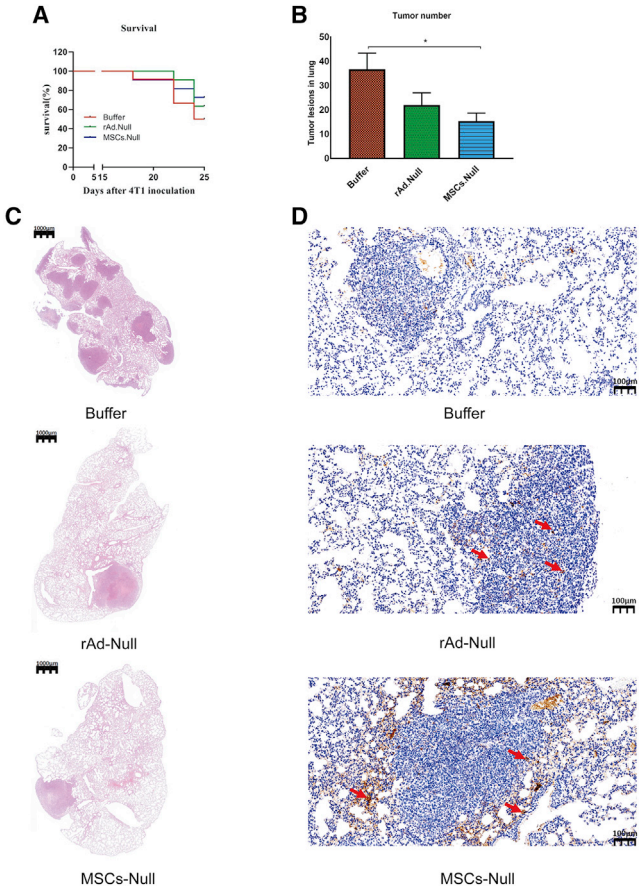

Figure 1. Therapeutic evaluation of oncolytic adenovirus rAd.Null-loaded mesenchymal stem cells in a breast cancer lung metastasis model

(A) The overall survival of mice. (B) On day 24, mice were euthanized, and the number of tumor metastatic lesions on the surface of lung was counted. (C) Representative images of hematoxylin and eosin (H&E) staining (scale bars: 1,000 μm). (D) The distribution of oncolytic adenoviruses was detected by immunohistochemistry using mouse anti-human adenovirus antibody, and representative images are shown (scale bars: 100 μm). Data in (B) are the mean ± SEM. *$p < 0.05$ versus the corresponding group.

In this study, we will evaluate the therapeutic responses of MSCs.DCN and MSCs.Null oncolytic adenovirus-loaded umbilical-cord-derived MSCs (UC-MSCs) in a breast cancer lung metastatic model.

RESULTS

Oncolytic adenoviruses could slightly replicate in UC-MSCs, lyse MSCs, and release viruses

To detect the replication of virus in UC-MSCs, 50% tissue culture infective dose (TCID50) was used to measure the viral titer of rAd.DCN collected from infected UC-MSCs. Replication of oncolytic adenoviruses, rAd.Null and rAd.DCN, was controlled by the TERT promoter. Here, we confirmed that oncolytic adenoviruses could slightly replicate in UC-MSCs and finally lyse MSCs and release viruses, and the viral titer increased with increasing time and the original infection titer (see also Figure S1). Therefore, UC-MSCs might be an ideal vehicle to deliver oncolytic adenovirus.

rAd.Null and rAd.DCN infection induces no changes in the immune phenotype of MSCs

The phenotype of MSCs infected with rAd.Null or rAd.DCN was analyzed by flow cytometry after staining with specific antibodies. The results showed that MSCs had characteristics of an immune phenotype, including the negative markers CD34 and human leukocyte antigen-DR (HLA-DR) and the positive markers CD73, CD90, and CD105, and oncolytic adenovirus infection did not change the immune phenotype of MSCs (see also Figure S2).

rAd.Null and rAd.DCN infection induces cytotoxic effects in breast cancer cells

Three cultured breast cancer cell lines, human MCF-7, MDA-MB-231, and murine 4T1, were infected with different titers of rAd.Null and rAd.DCN for 7 days, and crystal violet staining was performed to evaluate cytotoxic effects. The results demonstrated that human MCF-7, MDA-MB-231, and murine 4T1 cells were susceptible to killing by rAd.Null or rAd.DCN, and the killing efficiency was enhanced by increasing the virus infection titer. The cytotoxic effects were more robust in human MCF-7 and MDA-MB-231 cells than in 4T1 cells, and the cytotoxic effects were not significantly different between rAd.Null and rAd.DCN infection (see also Figure S3).

MSCs loaded with oncolytic adenovirus rAd.Null (MSCs.Null) could produce better antitumor effects than rAd.Null in a lung metastatic model

In this study, we used UC-MSCs as carriers to systemically deliver the oncolytic adenovirus rAd.Null in a mouse breast cancer lung metastasis model. We found that both MSCs.Null and rAd.Null improved the survival of 4T1-bearing mice; however, much more impressive responses could be observed in the MSCs.Null-treated group (Figure 1A). Importantly, hematoxylin and eosin (H&E) staining showed that both the MSCs.Null and rAd.Null groups had significantly fewer metastatic lesions in the lung than the buffer group (Figures 1B and 1C).

Moreover, the distribution of oncolytic adenoviruses in the lung was analyzed by immunohistochemistry. The results indicated that obvious oncolytic adenoviruses could be detected in tumor sites after treatment with MSCs.Null and rAd.Null. Compared with rAd.Null, MSCs.Null could enhance the load of oncolytic adenovirus in tumor tissues, suggesting that MSCs could target tumor tissues and deliver oncolytic adenoviruses effectively (Figure 1D). We also found rAd.Null could penetrate into the tumor tissues, while MSCs.Null could just reach the tumor periphery. In addition, the uptake of oncolytic adenoviruses in the liver was analyzed by immunohistochemistry. The results indicated that, compared with rAd.Null, MSCs.Null could significantly reduce the distribution of oncolytic adenovirus in the liver (see also Figure S4). Overall, MSCs might be an ideal vehicle to deliver oncolytic adenovirus.

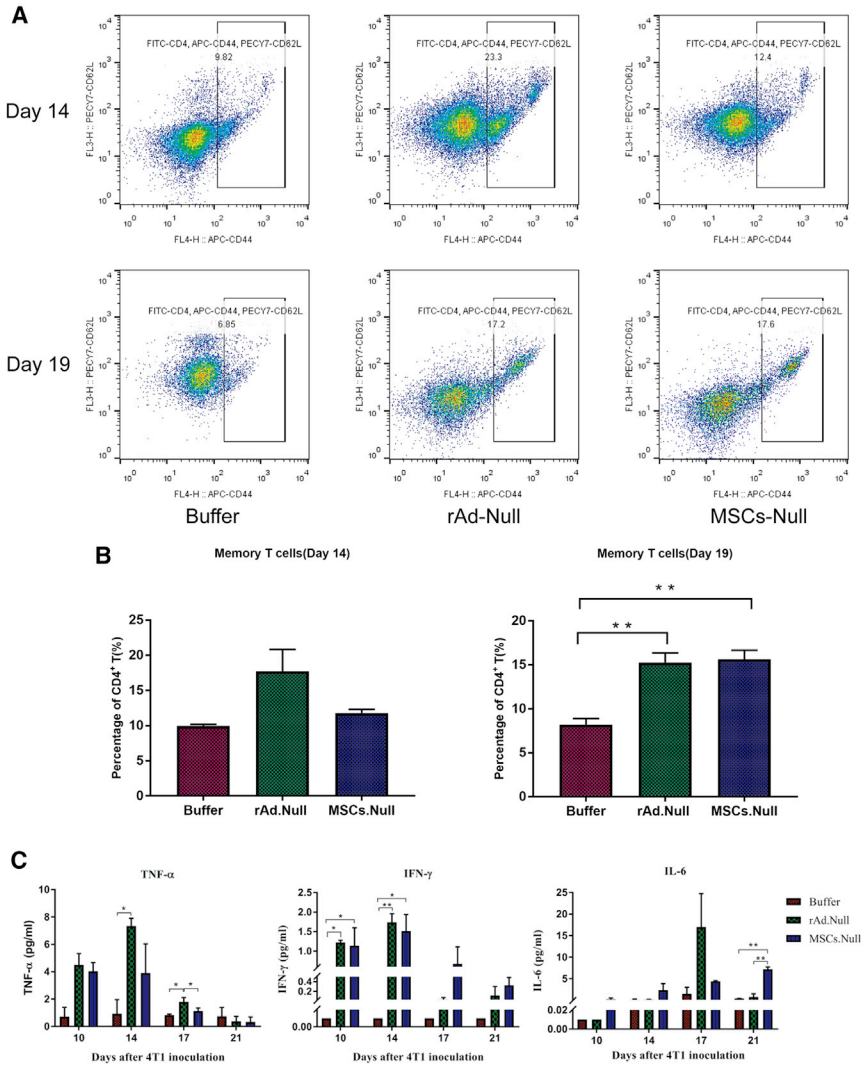

Figure 2. MSCs.Null and rAd.Null enhanced antitumor responses in peripheral blood

(A) The $CD4^+CD44^{High}CD62L^+$ memory T cells were analyzed by flow cytometry on days 14 and 19. (B) The statistical results of flow cytometry detection. (C) The protein concentrations of mouse interleukin-6 (IL-6), TNF-α, and IFN-γ were measured using the CBA Mouse Flex Set for IL-6, IFN-γ, and TNF-α (BD Biosciences) and analyzed by flow cytometry on days 10 and 17. Data are the mean ± SEM. *p < 0.05 and **p < 0.01 versus the corresponding group.

MSCs.Null and rAd.Null evoked obvious antitumor responses in peripheral blood

To evaluate the activation of antitumor immune responses, we analyzed the immune phenotypes of T lymphocytes and cytokine levels in peripheral blood by flow cytometry. On day 14, rAd.Null could increase the percentage of $CD44^+CD62L^+$ memory T cells among $CD4^+$ T lymphocytes, which might be attributed to the ability of rAd.Null to induce an anti-virus response. On day 19, both rAd.Null and MSCs.Null treatments improved the percentage of memory T cells, suggesting the activation of antitumor responses induced by rAd.Null or MSCs.Null (Figures 2A and 2B). Moreover, both rAd.Null and MSCs.Null treatments effectively promoted the expression and secretion of Th1 inflammatory cytokines, such as tumor necrosis factor alpha (TNF-α), interferon γ (IFN-γ), and interleukin-6 (IL-6) (Figure 2C). These results indicated that rAd.Null and MSCs.Null could evoke obvious antitumor responses in peripheral blood.

MSCs loaded with the oncolytic adenovirus carrying DCN could play negative roles in antitumor immune responses

Decorin, a natural inhibitor of TGF-β, could also target and inhibit tumor distal metastasis-related signaling pathways, such as Met, wnt/β-catenin, and VEGF. In our previous studies, we have reported that rAd.DCN can inhibit tumor growth and lung metastasis of breast cancer in both a bone metastatic model and an orthotopic model.[14,15] Here, in the 4T1 lung metastasis model, we also showed that rAd.DCN treatment improved the survival of mice and reduced metastatic lesions in the lung. As described above, MSCs.Null also evoked obvious antitumor responses, such as an increase in overall survival and inhibition of tumor dissemination. Interestingly, MSCs.DCN only slightly improved the survival (Figure 3A). Compared with MSCs.Null, MSCs.DCN significantly increased the number of tumor lesions in the lung (Figures 3B and 3C).

These findings suggested that decorin might play unexpected roles in antitumor responses via other mechanisms.

MSCs.DCN effectively produces decorin, delivers oncolytic adenovirus, recruits immune cells, and downregulates the expression of Th2 cytokines in the lung

The biological effects of MSCs loaded with oncolytic adenovirus in metastatic tumor sites were analyzed. Compared with intravenous injection of rAd.DCN, MSC-mediated delivery of rAd.DCN (MSCs.DCN) improved decorin expression in the lung (Figure 4A). As expected, rAd.DCN significantly reduced CTNNB1, a pivotal molecule of β-catenin signaling, and VEGFA in the lung. However, MSCs.DCN only slightly downregulated VEGFA expression. Moreover, both MSCs.DCN and MSCs.Null treatments improved Met expression (Figure 4A). These results suggested that oncolytic adenoviruses delivered by MSCs significantly blocked the inhibitory effects of decorin on the Met and wnt/β-catenin signaling pathways.

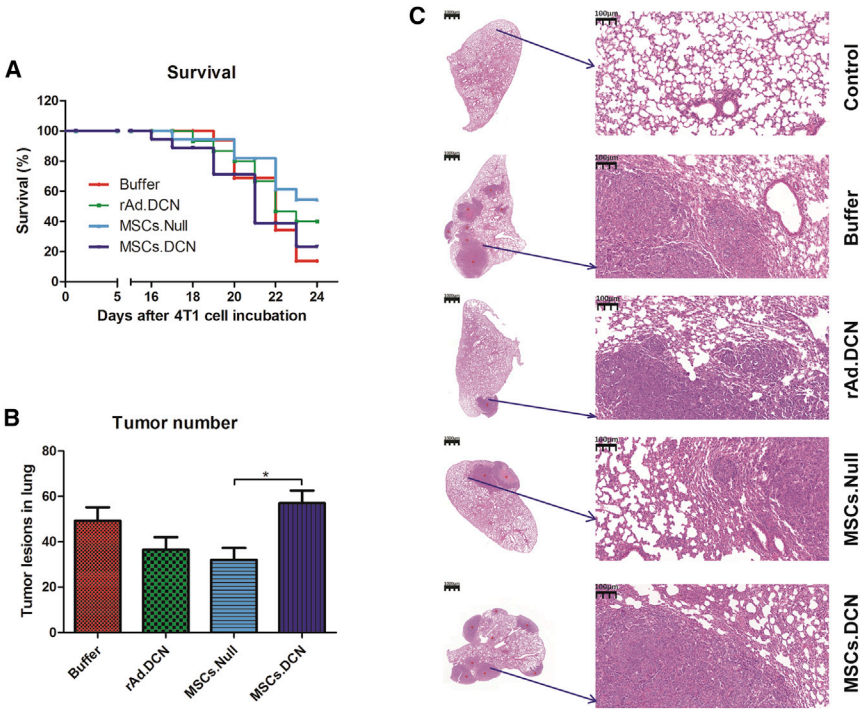

Figure 3. Therapeutic evaluation of oncolytic adenovirus rAd.DCN-loaded mesenchymal stem cells in a breast cancer lung metastasis model

(A) Overall survival of mice. (B) On day 24, mice were euthanized and the number of tumor metastatic lesions on the surface of lung was counted. (C) The tumor size was observed by histopathological analysis, and the representative images of H&E staining are shown (scale bars: left panel1,000 μm;right panel 100 μm). Data in (B) are the mean ± SEM. *p < 0.05 versus the corresponding group.

Aggregation of lymphocytes in tumor lesions is crucial for evoking effective antitumor immune responses. Immunohistochemical analysis indicated that rAd.DCN, MSCs.Null, and MSCs.DCN significantly increased the recruitment of $CD3^+$ T lymphocytes (Figure 4B, middle panel) and $CD68^+$ macrophages (Figure 4B, right panel) in the tumor microenvironment.

Furthermore, both MSCs.DCN and MSCs.Null obviously inhibited the expression of Th2 cytokines, such as TGF-β, IL-6, and IL-10, consistent with our previous reports showing that intravenous administration of rAd.DCN could reduce the expression of Th2 cytokines. These findings indicated that MSC-mediated delivery of oncolytic adenovirus could improve the tumor microenvironment. However, MSCs.Null inhibited TGF-β and IL-10 expression much more strongly than MSCs.DCN in the lung (Figure 4C).

MSCs.DCN inhibits the activation of antitumor immune responses via various mechanisms in peripheral blood

Then, the immune phenotypes of T lymphocytes in peripheral blood were analyzed. Our data showed that rAd.DCN slightly downregulated the percentage of $CD25^+FoxP3^+$ regulatory T cells (Treg cells), while MSCs.DCN and MSCs.Null treatments increased Treg cells (Figure 5A). Moreover, rAd.DCN treatment could upregulate T memory cells in peripheral blood, but MSCs.DCN treatment slightly reduced the percentage of these cells (Figure 5A). These results implied that MSCs might inhibit antitumor immune responses in peripheral blood.

We also analyzed the expression of cytokines in peripheral blood by flow cytometry. The results showed that rAd.DCN treatment effectively improved the expression of Th1 cytokines (Figure 5B), such as IL-2, IL-9, and IL-12, as well as the Th2 cytokine IL-10. In contrast, compared with rAd.DCN treatment, MSC-mediated delivery of oncolytic adenoviruses, especially MSCs.DCN, could not only suppress the levels of Th1 cytokines (Figure 5B) but also significantly increased the levels of Th2 cytokines (Figure 5C). Our findings suggested that, in peripheral blood, MSCs played a negative role in activating antitumor immune responses, and overexpression of decorin in MSCs could enhance these inhibitory effects.

MSCs.DCN promotes the migration of 4T1 cells by upregulating Met, β-catenin, and VEGF signaling

To explore the mechanisms under failure of MSCs.DCN in the treatment of the 4T1 lung metastasis mouse model, we cocultured 4T1 cells with oncolytic-adenovirus-loaded MSC or MSC lysates and detected the expression of decorin and its target genes. Surprisingly, we observed that these two different coculture methods caused completely contrary results. The MSCs.DCN lysate significantly downregulated the expression of Met, CTNNB1, and VEGFA compared with the MSCs.Null lysate, which might be due to the high concentration of decorin protein in the lysate (Figure 6A). However, compared with the treatment with cocultured MSCs.Null, MSCs.DCN clearly increased the expression of Met, CTNNB1, and VEGFA (Figure 6B). Therefore, we hypothesized that the activation of some cell-contact-dependent signaling mechanisms might be attributed to unexpected inhibitory effects of MSCs.DCN on tumor growth and metastasis.

DISCUSSION

Oncolytic viruses have become an alternative immune therapy for tumors. Oncolytic viruses can not only directly lyse tumor cells via viral replication but also activate antitumor immune responses by releasing a large amount of tumor antigens and regulating the tumor microenvironment. Talimogene laherparepvec (T-Vec), an oncolytic herpes simplex virus type 1 expressing

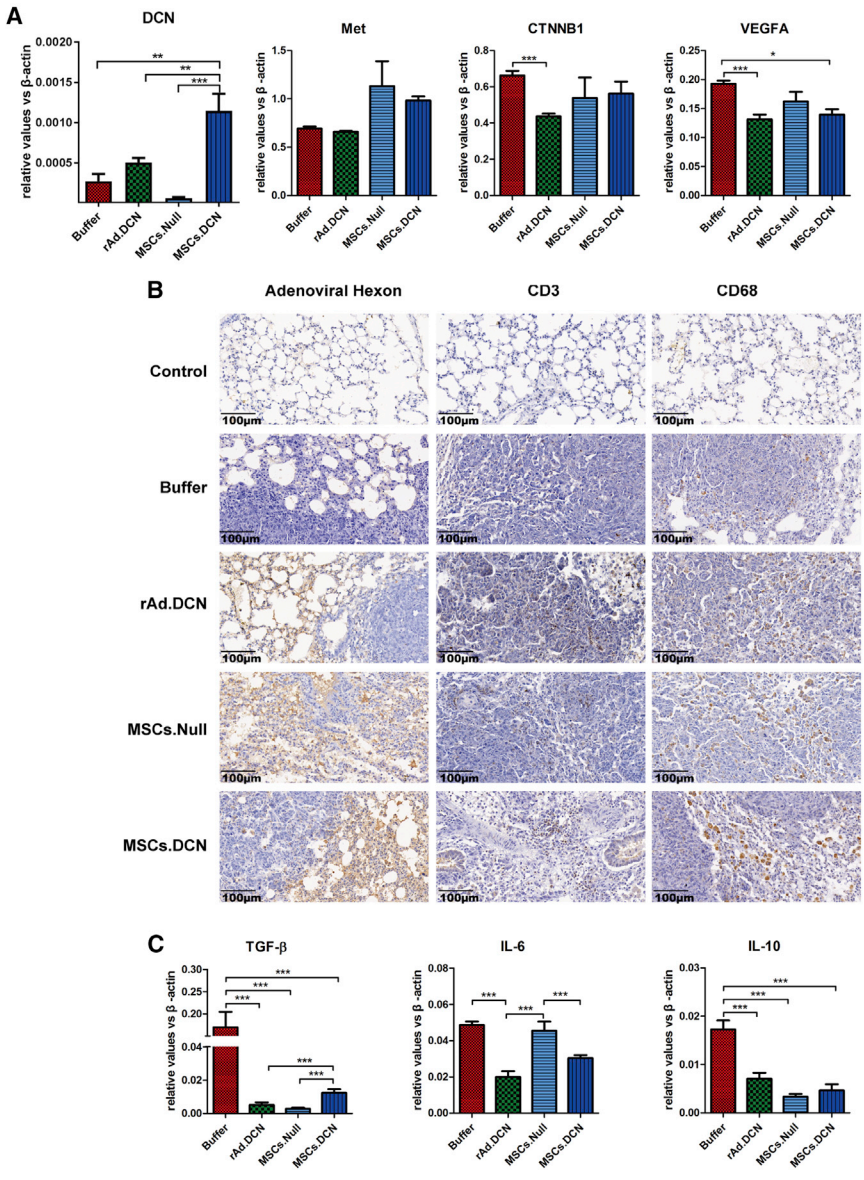

Figure 4. MSCs.DCN effectively produces decorin, delivers oncolytic adenovirus, recruits immune cells, and downregulates the expression of Th2 cytokines in the lung

(A) The expression levels of human decorin, mouse Met, mouse CTNNB1, and mouse vascular endothelial growth factor A (VEGFA) in lung were detected by real-time reverse-transcriptase polymerase chain reaction (RT-PCR) on day 24. (B) The lung tissues were processed for histopathological analysis. The distribution of oncolytic adenoviruses was detected by immunohistochemistry using mouse anti-human adenovirus antibody (left panel). The infiltration of $CD3^+$ T lymphocytes (middle panel) and $CD68^+$ macrophages (right panel) was also analyzed by immunohistochemistry using anti-CD3 and anti-CD68, respectively. Representative images are shown (scale bars: 100 μm). (C) The expression of Th2 cytokines, such as transforming growth factor β (TGF-β), IL-6, and IL-10, in lung was also analyzed by real-time PCR. Data are the mean ± SEM. *$p < 0.05$, **$p < 0.01$, and ***$p < 0.001$ versus the corresponding group.

granulocyte-macrophage colony stimulating factor (GM-CSF), was approved by the USA Food and Drug Administration (FDA) for treating advanced melanoma in 2015.[26,27] In recent years, our group has focused on the application of TGF-β-signaling-targeted oncolytic adenoviruses, such as oncolytic adenovirus overexpressing soluble TGF-β receptor II-Fc fusion protein (sTGFbRIIFc) or decorin,[14,15,28,29] to treat distal tumor metastasis. The ideal mode of oncolytic viral delivery to reach the distal tumor metastasis area is systemic administration via vein injection. However, liver uptake and immune neutralization are two major barriers to utilizing Ad5-based oncolytic adenoviruses *in vivo*.[30–32] Some studies, including our group's former research, have reported that modification of the hexon gene of Ad5 can reduce liver uptake and neutralize the immune system.[33–35] However, further improvements are needed before application to clinical therapy.

In recent years, MSCs have emerged as effective carriers for gene delivery in the treatment of various diseases, including cancer therapy.[19,21,36] However, MSCs have multiple biological functions, and the effect of MSCs on the growth and metastasis of tumors is controversial. Some studies have reported that MSCs can improve antitumor responses,[37,38] and the delivery of oncolytic viruses by MSCs not only can prevent potential promotive effects on tumor growth and metastasis by lysing MSCs but also abate antibody neutralization, increase intratumoral accumulation of oncolytic viruses, and finally enhance antitumor responses.[39–41] Some research has reported that MSCs can support tumor growth and progression by secreting growth factors and inhibiting antitumor immune and inflammatory responses.[42,43]

Decorin is a member of the small leucine-rich proteoglycan family, which was initially identified as an inhibitor of the TGF-β signaling pathway.[44] TGF-β is a pivotal molecule that can regulate the tumor microenvironment and play a negative role in antitumor responses; for example, it can suppress the maturation of dendritic cells (DCs), T helper lymphocytes (Th), and natural killer cells (NK); facilitate M2 polarization of macrophage cells; and induce the Th1/Th2 balance toward the Th2 immune phenotype.[45–47] We have previously reported that an oncolytic adenovirus encoding decorin can motivate

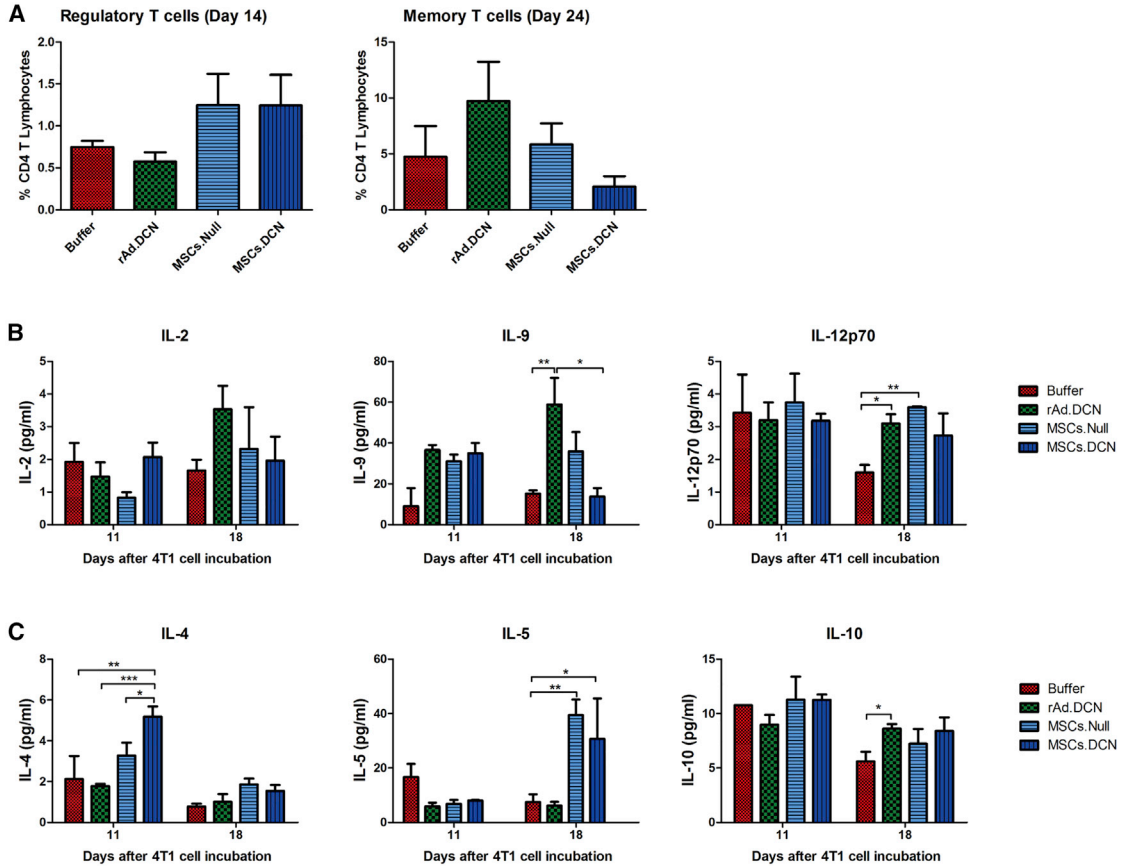

Figure 5. Oncolytic adenovirus-loaded MSCs regulate immune activation in peripheral blood

(A) On day 14, EDTA-anticoagulated peripheral blood samples were collected. In addition, $CD4^+CD25^+FoxP3^+$ regulatory T cells (Treg cells) were labeled and analyzed by flow cytometry on day 14. The percentage of Treg cells among $CD4^+$ T lymphocytes was calculated and is presented (left panel). The $CD4^+CD44^{High}CD62L^+$ memory T cells were analyzed by flow cytometry on day 24, and the statistical results are shown (right panel). (B) The protein concentration of Th1 cytokines in sera, including mouse IL-2, mouse IL-9, and mouse IL-12p70, were measured on days 11 and 18 using the mouse Th1/Th2/Th9/Th17/Th22/Treg cell cytokine panel 1 and analyzed by MagPix. (C) The protein concentration of Th2 cytokines, such as IL-4, IL-5, and IL-10, were measured and analyzed using the same method as described for the Th1 cytokines. Data are the mean ± SEM. *$p < 0.05$, **$p < 0.01$, and ***$p < 0.001$ versus the corresponding group.

antitumor immune responses by increasing Th1 cytokines and downregulating Th2 cytokines.[14,29]

In this study, we delivered the oncolytic adenovirus rAd.Null and rAd.DCN by UC-MSCs to treat breast cancer lung metastasis in a mouse model. The experiments were mainly composed of two parts: evaluating the biological effects of using MSCs as oncolytic adenovirus carriers and loading decorin in oncolytic adenoviruses.

In the first part, we found that both naked oncolytic adenoviruses rAd.Null and MSCs.Null could achieve positive therapeutic effects by evoking antitumor responses in peripheral blood, including increasing the percentage of memory T cells and promoting the expression of inflammatory cytokines, such as TNF-α, IFN-γ, and IL-6. More importantly, in comparison to directly injecting oncolytic adenoviruses intravenously, MSCs.Null improved the viral quantity and distribution in tumor tissues on day 24, indicating that MSCs could be used to load and deliver oncolytic adenovirus. This method of delivery can overcome the shortcomings of the traditional intratumoral injection route, significantly improving infection efficiency and tumor targeting.

In the second part, we found that oncolytic adenoviruses encoding decorin (rAd.DCN) delivered by MSCs (MSCs.DCN) exerted complicated biological effects. MSCs.Null, but not MSCs.DCN, induced significant antitumor responses by activating tumor immune responses. Although both MSCs.Null and MSCs.DCN reduced the expression of Th2 cytokines, such as TGF-β and IL-10, MSCs.Null caused a much more impressive downregulation of TGF-β and IL-10 in the lung. These results suggested that the inhibitory effects of decorin on Th2 cytokine expression were abolished when tumor cells contacted MSCs.DCN by activating contact-dependent mechanisms.

In addition to immune regulatory function, decorin could also inhibit tumor growth and metastasis by targeting and blocking pivotal molecules, such as Met, wnt/β-catenin, and VEGF,[9,10] which are associated with cancer metastasis. Some studies have shown that, in metastatic models of breast cancer or colorectal cancer, oncolytic adenovirus encoding decorin (rAd.DCN) obviously downregulated the expression of Met, CTNNB1, and VEGFA.[14,15,29] Furthermore, due to the lysis effect on tumor cells, the oncolytic adenovirus itself could reduce the expression of Met, CTNNB1, and VEGFA.

Intriguingly, in our *in vitro* experiment, treatment with lysates from MSCs.DCN inhibited the expression of Met, CTNNB1, and VEGFA in 4T1 cells. However, no obvious decrease in Met and CTNNB1 was detected in 4T1 cells after coculture with MSCs.Null or MSC.DCN. Moreover, coculture with MSCs.DCN even upregulated their expression in 4T1 cells. These results were consistent with the regulatory effect of MSCs.DCN in the tumor immune microenvironment, suggesting that the contact of MSCs.DCN with tumors could cause adverse effects on antitumor responses.

As described in the materials and methods, the replication of oncolytic adenoviruses, rAd.Null and rAd.DCN, was controlled by the TERT promoter. Our *in vitro* experiments showed that oncolytic adenoviruses could replicate slightly in umbilical-cord-derived MSCs and finally lyse MSCs to release viruses (see also Figure S1). In conclusion, MSCs might be an ideal vehicle to deliver the oncolytic adenovirus rAd.Null and rAd.DCN-loaded MSCs, and MSCs.Null and MSC.DCN could improve the delivery efficiency of oncolytic adenoviruses. However, MSCs loaded with the oncolytic adenovirus carrying DCN could play negative roles in antitumor immune responses, and the contact of breast cancer cells with MSCs.DCN not only abolished the inhibitory effects of decorin and oncolytic adenoviruses on Th2 cytokine expression but also reversed the regulatory roles of Met, CTNNB1, and VEGFA, which are pivotal molecules in tumor-metastasis-associated signaling pathways.

A rather recent report dealing with MSC-mediated intravenous delivery of oncolytic viral constructs in mice bearing melanoma lung lesions obtained some similar results to our research: using MSCs as carriers to deliver oncolytic viruses can increase the accumulation and persistence of viruses in the lungs of lesion-bearing mice;[48] moreover, this therapy can enhance the therapeutic effect *in vivo* to some extent, suggesting that MSCs would be safe and efficient for therapeutic oncolytic viruses. A discrepancy is that IL-15-expressing MYXV delivered by MSCs can reduce tumor burden and obtain some positive effects; however, DCN-expressing oncolytic adenoviruses delivered by MSCs cause adverse effects on antitumor responses, possibly via a contact-dependent mechanism. This discrepancy may result from the difference in loaded genes, which play a distinct function in the regulation of the antitumor response. For instance, the IL-15-expressing MYXV construct has been reported to dramatically increase the accumulation of NK cells in tumors. But MSCs.DCN obviously increased the expression of Met, CTNNB1, and VEGFA and inhibited the activation of antitumor immune responses via various mechanisms in peripheral blood. We hypothesized that the activation of some cell-contact-dependent signaling mechanisms might be attributed to the unexpected inhibitory effects of MSCs.DCN on tumor growth and metastasis.

The interaction between MSCs and oncolytic adenoviruses encoding some genes is complicated, so further investigations should be conducted to clarify the underlying mechanisms and explore a more beneficial MSC-mediated oncolytic adenoviral therapy.

MATERIALS AND METHODS

Ethics statement

BALB/c mice were purchased from Beijing Vital River Laboratory Animal Technology (Beijing, China). Animal experiments were approved by the Institutional Animal Care and Use Committee of Laboratory Animal Center (IACUC-DWZX-2020-706).

Cell lines

The mouse breast cancer cell line (4T1) was obtained from American Type Culture Collection (ATCC) (Manassas, VA, USA). The lentiviral vector encoding luciferase was transduced into 4T1 cells to generate 4T1-Luc cells. Both 4T1 and 4T1-Luc cells were maintained in RPMI-1640 (Gibco, Gaithersburg, MD) supplemented with 10% fetal calf serum (FCS) (HyClone, Logan, UT).

Human umbilical cords were obtained from the Fifth Medical Center of PLA General Hospital with written informed consent from the parturient. UC-MSCs were isolated as described previously[49] and maintained in α-minimum essential medium (α-MEM) (Gibco, Gaithersburg, MD) supplemented with 10% FCS (HyClone, Logan, UT), and their immune phenotypes (positive for CD73, CD90, and CD105 and negative for CD34, CD45, and HLA-DR) were identified by flow cytometry. Moreover, multidifferentiation characteristics of MSCs, including adipocytic and osteogenic differentiation, were also detected (data not shown). Cells were collected at passages 4 to 5 for the study experiments.

Adenoviruses

Oncolytic adenovirus expressing decorin (rAd.DCN) and control oncolytic adenovirus (rAd.Null), of which viral replication was controlled by the telomerase reverse transcriptase (TRET) promoter, were prepared as described previously.[29] The oncolytic adenoviruses were purified by CsCl density gradient ultracentrifugation. Viral particle (vp) numbers and viral infectious titers (infectious units [IUs] per milliliter) were determined by spectrophotometry and the TCID50, respectively, as previously described.[29] The infection intensity multiplicity of infection (MOI) was calculated from the infectious titers.

UC-MSCs were infected with rAd.Null or rAd.DCN at 10 MOI to generate oncolytic-adenovirus-loaded MSCs (MSCs.Null or MSCs.DCN). Three hours after infection, the culture media were discarded, the cells were washed twice with PBS, and fresh culture media

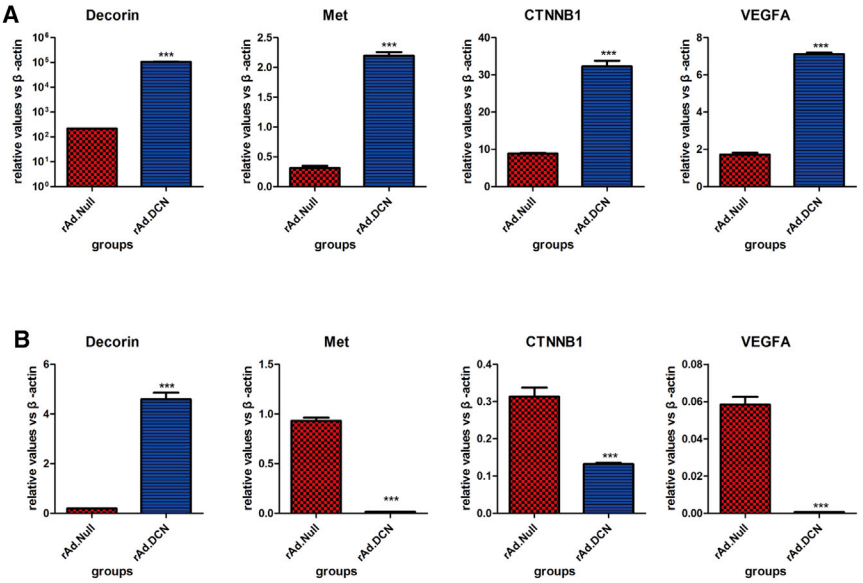

Figure 6. Effects of oncolytic-adenoviruses-loaded MSCs on the expression of metastatic-related molecules in 4T1 cells *in vitro*

The 4T1 cells were seeded on MSCs.DCN or MSCs.Null (A) or their lysates (B) were added to 4T1 cells. After co-culturing or stimulating for 5 days, the mRNA expression levels of human decorin, mouse Met, mouse CTNNB1, and VEGFA were analyzed by real-time RT-PCR. Data are the mean ± SEM. ***$p < 0.001$ versus the corresponding group.

were added. Twenty-four hours postinfection, the cells were collected for therapy in animal models.

Analysis of viral replication in MSCs

To detect the replication of oncolytic adenovirus in MSCs, UC-MSCs were seeded into 6-well plates at a density of 4×10^5 cells per well and infected with rAd.DCN at different titers (MOI = 0, 5, 10, and 20). Four hours later, the inoculum was removed, the cells were washed twice with PBS, fresh medium was added for further incubation (5% CO2, 37°C), and the cells and supernatant were collected at 2, 5, and 7 days after infection. Then, cells or supernatants were frozen and thawed three times between 37°C and −80°C to release the virus. Following centrifugation (10,000 rpm, 5 min), the supernatant was collected and titrated back to 293 cells (1×10^4 cells per well of a 96-well plate) by serial dilutions. Cytopathic effects (CPEs) were observed using an inverted microscope (Olympus, Japan) at 10 days after infection. Titers (IU per milliliter) were calculated according to the following equation:

$$\text{virus titres} = \frac{\text{the number of well occuring CPEs at the highest dilution factor} \times \text{the dilution factor}}{\text{volume of the supernatant at this dilution}}$$

Flow cytometry analysis of the immune phenotype of MSCs after infection with oncolytic adenovirus

To detect the immune phenotype change of MSCs caused by oncolytic adenovirus infection, cultured MSCs (4×10^5 cells per well of a 6-well plate) were infected with rAd.Null or rAd.DCN (MOI = 10). Four hours later, the inoculum was removed with fresh medium or not removed, and the cells were further incubated (5% CO2, 37°C) for 48 h. Next, the cells were trypsinized and washed twice with 2 mL PBS, followed by incubation with appropriate antibodies against CD73-phycoerythrin (PE), CD90-antigen-presenting cell (APC), CD105-PECY7, CD34-fluorescein isothiocyanate (FITC), and HLA-DR-FITC (Thermo Fisher Scientific, CA) for 40 min at room temperature. Ultimately, the cells were washed twice with 2 mL PBS, suspended in 400 μL PBS, and analyzed on a BD FACSCanto II flow cytometer (Becton-Dickinson, Franklin Lakes, NJ, USA). Noninfected cells were used as a control, and cells without antibody staining were used as a blank.

Analysis of cytotoxic effects of rAd.Null and rAd.DCN infection

To detect the cytotoxic effects of oncolytic adenovirus on breast cancer cell lines, three cultured breast cancer cell lines (human MCF-7, MDA-MB-231, and murine 4T1) were infected with oncolytic adenovirus at different titers of rAd.Null (MOI = 20, 10, 1, 0.1, 0.01, and 0) or rAd.DCN (MOI = 20, 10, 1, 0.1, 0.01, and 0), and the cytotoxic effects were evaluated by crystal violet staining. Briefly, cells in medium were seeded into 96-well plates at a density of 1×10^4 cells per well and then infected with oncolytic adenovirus at different titers (in quintuplicate) for 7 days. The cells were then fixed with 1% glutaraldehyde for 2 h and stained with 0.1% crystal violet solution (Servicebio, Wuhan, China) for 1 h at room temperature. Subsequently, the crystal violet solution was removed, and the cells were washed twice with distilled water and dried in air. Then, the samples were dissolved in 1% Triton X-100, and the fluorescent signal (emission = 570 nm) was measured using a Varioskan Flash plate reader (Thermo Fisher

Scientific, US). The killing efficiency of a virus was calculated according to the following formula:

$$\text{killing efficiency} = \frac{1 - \text{A570nm of virus infected well}}{\text{volume of the supernatant at this dilution}}$$

The data are presented as the means ± SD for individual time points.

Establishment of the breast cancer lung metastasis model

To establish a breast cancer lung metastasis model, 2×10^5 4T1-Luc cells per 100 μL PBS were injected intravenously into 6- to 8-week-old female BALB/c mice. Seven days after injection, tumor lung metastasis was confirmed by real-time bioluminescence imaging (BLI) (see also Figure S5).

Therapy with oncolytic adenovirus and MSCs

First, to assess the therapeutic effects of oncolytic adenovirus delivered by MSCs, tumor-bearing mice were divided into three groups without significant differences (n = 12/group). In addition, 2.5×10^{10} vps rAd.Null per 100 μL PBS (rAd.Null group), 1.0×10^6 MSCs.Null (MSCs.Null group) per 100 μL PBS, and 100 μL PBS (buffer group) was administered intravenously for therapy. The survival of the mice was monitored daily, and the mice were euthanized to analyze lung metastatic lesions 24 days after model establishment.

Second, to assess the therapeutic effects of the oncolytic adenovirus encoding decorin, tumor-bearing mice were divided into four groups without significant differences (n = 15/group). In addition, 2.5×10^{10} vps rAd.DCN per 100 μL PBS (rAd.DCN group), 1.0×10^6 MSCs.Null (MSCs.Null group) or MSCs.DCN (MSCs.DCN group) per 100 μL PBS, and 100 μL PBS (buffer group) were administered intravenously for therapy. The survival of mice was monitored daily, and the mice were euthanized to analyze lung metastatic lesions 24 days after model establishment.

Histopathological analysis and immunohistochemistry

On day 24, mice from each group were euthanized. The lungs and livers were harvested, and the tumor metastatic lesions in the lung were counted. Then, the lung tissues were processed and stained with H&E. Moreover, the distribution of oncolytic adenoviruses in the lung was analyzed by immunohistochemistry using a mouse anti-adenovirus antibody (Abcam, Cambridge, MA) and a goat anti-human decorin antibody (R&D Systems, Minneapolis, MN). Furthermore, the infiltration of lymphocytes, including $CD3^+$ T lymphocytes and macrophages, was also detected by immunohistochemistry using rabbit anti-mouse CD3 (Abcam, Cambridge, MA) and rabbit anti-mouse CD68 (Servicebio, Wuhan, China), respectively. Horseradish peroxidase (HRP)-conjugated rabbit anti-goat immunoglobulin G (IgG) (Servicebio, Wuhan, China) or HRP-conjugated goat anti-rabbit IgG was used as the secondary antibody (Servicebio, Wuhan, China).

Immune phenotypes of T lymphocytes in peripheral blood

On days 14, 19, and 24, EDTA-anticoagulated peripheral blood samples were collected to analyze subtypes of T lymphocytes, including Treg cells and memory T cells.

For Treg cells, blood samples were labeled with FITC-conjugated mouse CD4 antibody and PE-conjugated mouse CD25 antibody (Thermo Fisher Scientific, CA) for 20 min. After lysis in 1× red blood cell (RBC) lysis buffer, fixation and permeabilization procedures were conducted. Then, the cells were labeled with APC-conjugated mouse Foxp3 antibody and analyzed by flow cytometry.

For memory T cells, blood samples were stained with APC-conjugated rat anti-mouse CD44 antibody (APC-CD44), FITC-conjugated rat anti-mouse CD4 antibody (FITC-CD4), PE-conjugated rat anti-mouse CD62L antibody (PE-CD62L), and PerCP-Cyanine5.5-conjugated rat anti-mouse CD3e antibody (PerCP-Cy5.5-CD3e; PeproTech, Rocky Hill, NJ). The percentages of memory T cells were detected by flow cytometry after RBC lysis.

Inflammatory cytokine levels in peripheral blood

On days 10 and 17, peripheral blood samples were treated as described previously. The concentrations of IL-6, IFN-γ, and TNF-α were measured using a CBA Mouse Flex Set for IL-6, IFN-γ, and TNF-α (BD Biosciences). Briefly, 50 μL of the mixed capture beads and 50 μL of serum were incubated for 1 h at room temperature, and after adding 50 μL of the mixed PE detection reagent to the mixture, it was incubated for 2 h at room temperature. The beads were then washed with wash buffer and analyzed with FACSCalibur (BD Biosciences). The CBA data were analyzed with FlowJo software version 10.

On days 10, 14, 17, 18, and 21, peripheral blood samples were collected from each group. The sera were collected by centrifugation after incubation at 37°C for 30 min and at 4°C for 60 min. The protein concentrations of mouse IL-2, IL-4, IL-5, IL-6, IL-9, IL-10, IL12p70 (IL-12p70), TNF-α, and IFN-γ were measured using the mouse Th1/Th2/Th9/Th17/Th22/Treg cell cytokine panel 1 (17 plex; Thermo Fisher Scientific, CA) and analyzed by Multi Sciences (Hangzhou, China).

Analysis of decorin and its target genes and Th2 cytokine expression in lung tissues

On day 24, the mice were euthanized and the lungs were removed. Total RNA was isolated, and complementary cDNA was synthesized. The mRNA expression of decorin, decorin target genes (Met, CTNNB1, and VEGFA), and Th2 cytokines (TGF-β, IL-6, and IL-10) was analyzed by real-time RT-PCR.

Analysis of decorin and its target gene expression *in vitro*

Oncolytic-adenovirus-loaded MSCs, MSCs.DCN and MSCs.Null, were generated by transducing UC-MSCs with 10 MOI rAd.DCN and rAd.Null, respectively. Lysates of MSCs.DCN and MSCs.Null were prepared by repeated freezing and thawing three times. The

Table 1. Real-time RT-PCR primers

Gene	Direction	Sequence (5′-3′)
Actin-mouse	forward	AGGCCAACCGTGAAAAGATG
	reverse	TGGCGTGAGGGAGAGCATAG
Decorin-human	forward	GGGATAGGCCCAGAAGTT
	reverse	TGGCATTGACAGCGGAAG
Met-mouse	forward	CCGTAGACTCTGGGTTGC
	reverse	ATCTGGCTTGCTTTGTGC
CTNNB1-mouse	forward	GGGTGCTATTCCACGACT
	reverse	CCCTTCTACTATCTCCTCCAT
VEGFA-mouse	forward	CTGCCGTCCGATTGAGACC
	reverse	CCCCTCCTTGTACCACTGTC
TGF-β-mouse	forward	CTCCCGTGGCTTCTAGTGC
	reverse	GCCTTAGTTTGGACAGGATCTG
IL-6-mouse	forward	GCTACCTGGAGTACATGAAGAACA
	reverse	GGTCCTTAGCCACTCCTTCTG
IL-10-mouse	forward	AGTGGTATAGACAGGTCTGTTGG
	reverse	GCAGCTCTAGGAGCATGTGG

4T1 cells were seeded at a density of 1.5×10^5 cells per well per mL media and then cocultured with MSC lysates from 3×10^5 MSCs.Null and MSCs.DCN or cocultured with 3×10^5 MSCs.Null and MSCs.DCN cells. After coculture for 5 days, the cells were collected and total RNA was extracted. After cDNA was synthesized, the mRNA expression levels of human decorin, mouse Met, mouse CTNNB1, and VEGFA were analyzed by real-time RT-PCR.

Real-time RT-PCR

The mRNA expression of various genes was quantified using 2× RealStar Green Fast Mixture with ROX II (Genstar, China) on a 7500 Fast Real-Time PCR System (Applied Biosystems S/Life Technologies, Foster City, CA). The relative expression level was calculated by $2^{-\Delta CT}$ using mouse β-actin as a control. The primers used are listed in Table 1.

Statistical analysis

All data were analyzed using GraphPad Prism software v.5 (GraphPad Software, San Diego, CA) and expressed as the mean ± standard error of the mean. Longitudinal data (cytokine levels in sera) were analyzed using two-way repeated-measures ANOVA followed by Bonferroni post hoc tests. Others were analyzed by one-way ANOVA followed by Bonferroni post hoc tests. Differences were considered significant at a two-sided $p < 0.05$.

SUPPLEMENTAL INFORMATION

Supplemental information can be found online at https://doi.org/10.1016/j.omto.2022.01.007.

ACKNOWLEDGMENTS

This work was supported by the Natural Science Foundation of Zhejiang Province (no. LY19H160010) and the Opened-end Fund of Key Laboratory of Diagnosis and Treatment of Digestive System Tumors of Zhejiang Province, 2019E10020 (KFJJ-202003).

AUTHOR CONTRIBUTIONS

Y.Z. and C.L. wrote the paper. Y.Z., C.L., H.Z., J.Y., X.D., and F.X. conceived the experiments. T.W., H.D., and N.T. collected and provided the samples for the study. Y.Y. and H.W. designed the study and analyzed the data. All authors have read and approved the final submitted manuscript.

DECLARATION OF INTERESTS

The authors declare no competing interests.

REFERENCES

1. Bray, F., Ferlay, J., Soerjomataram, I., Siegel, R.L., Torre, L.A., and Jemal, A. (2018). Global cancer statistics 2018: GLOBOCAN estimates of incidence and mortality worldwide for 36 cancers in 185 countries. CA Cancer J. Clin. *68*, 394–424.
2. Chambers, A.F., Groom, A.C., and MacDonald, I.C. (2002). Dissemination and growth of cancer cells in metastatic sites. Nat. Rev. Cancer *2*, 563–572.
3. Xiao, W., Zheng, S., Liu, P., Zou, Y., Xie, X., Yu, P., Tang, H., and Xie, X. (2018). Risk factors and survival outcomes in patients with breast cancer and lung metastasis: a population-based study. Cancer Med. *7*, 922–930.
4. Fidler, I.J. (2003). The pathogenesis of cancer metastasis: the 'seed and soil' hypothesis revisited. Nat. Rev. Cancer *3*, 453–458.
5. Solomayer, E.F., Diel, I.J., Meyberg, G.C., Gollan, C., and Bastert, G. (2000). Metastatic breast cancer: clinical course, prognosis and therapy related to the first site of metastasis. Breast Cancer Res. Treat *59*, 271–278.
6. Wu, Q., Li, J., Zhu, S., Wu, J., Chen, C., Liu, Q., Wei, W., Zhang, Y., and Sun, S. (2017). Breast cancer subtypes predict the preferential site of distant metastases: a SEER based study. Oncotarget *8*, 27990–27996.
7. Medeiros, B., and Allan, A.L. (2019). Molecular mechanisms of breast cancer metastasis to the lung: clinical and experimental perspectives. Int. J. Mol. Sci. *20*, 2272.
8. Smid, M., Wang, Y., Zhang, Y., Sieuwerts, A.M., Yu, J., Klijn, J.G., Foekens, J.A., and Martens, J.W. (2008). Subtypes of breast cancer show preferential site of relapse. Cancer Res. *68*, 3108–3114.
9. Neill, T., Schaefer, L., and Iozzo, R.V. (2015). Oncosuppressive functions of decorin. Mol. Cell Oncol. *2*, e975645.
10. Neill, T., Painter, H., Buraschi, S., Owens, R.T., Lisanti, M.P., Schaefer, L., and Iozzo, R.V. (2012). Decorin antagonizes the angiogenic network: concurrent inhibition of met, hypoxia inducible factor 1α, vascular endothelial growth factor A, and induction of thrombospondin-1 and TIMP3. J. Biol. Chem. *287*, 5492–5506.
11. Neill, T., Schaefer, L., and Iozzo, R.V. (2012). Decorin: a guardian from the matrix. Am. J. Pathol. *181*, 380–387.
12. Neill, T., Schaefer, L., and Iozzo, R.V. (2016). Decorin as a multivalent therapeutic agent against cancer. Adv. Drug Deliv. Rev. *97*, 174–185.
13. Oh, E., Choi, I.K., Hong, J., and Yun, C.O. (2017). Oncolytic adenovirus coexpressing interleukin-12 and decorin overcomes Treg-mediated immunosuppression inducing potent antitumor effects in a weakly immunogenic tumor model. Oncotarget *8*, 4730–4746.
14. Zhao, H., Wang, H., Kong, F., Xu, W., Wang, T., Xiao, F., Wang, L., Huang, D., Seth, P., Yang, Y., et al. (2019). Oncolytic adenovirus rAd.DCN inhibits breast tumor growth and lung metastasis in an immune-Competent orthotopic xenograft model. Hum. Gene Ther. *30*, 197–210.
15. Yang, Y., Xu, W., Neill, T., Hu, Z., Wang, C.H., Xiao, X., Stock, S.R., Guise, T., Yun, C.O., Brendler, C.B., et al. (2015). Systemic delivery of an oncolytic adenovirus

expressing decorin for the treatment of breast cancer bone metastases. Hum. Gene Ther. *26*, 813–825.

16. Jang, Y.O., Kim, M.Y., Cho, M.Y., Baik, S.K., Cho, Y.Z., and Kwon, S.O. (2014). Effect of bone marrow-derived mesenchymal stem cells on hepatic fibrosis in a thioacetamide-induced cirrhotic rat model. BMC Gastroenterol. *14*, 198.
17. Avery, M.B., Belanger, B.L., Bromley, A., Sen, A., and Mitha, A.P. (2019). Mesenchymal stem cells exhibit both a proinflammatory and anti-inflammatory effect on saccular aneurysm formation in a rabbit model. Stem Cells Int. *2019*, 3618217.
18. Chen, H., Tang, S., Liao, J., Liu, M., and Lin, Y. (2019). Therapeutic effect of human umbilical cord blood mesenchymal stem cells combined with G-CSF on rats with acute liver failure. Biochem. Biophys. Res. Commun. *517*, 670–676.
19. Du, L., Liang, Q., Ge, S., Yang, C., and Yang, P. (2019). The growth inhibitory effect of human gingiva-derived mesenchymal stromal cells expressing interferon-β on tongue squamous cell carcinoma cells and xenograft model. Stem Cell Res. Ther. *10*, 224.
20. Timaner, M., Tsai, K.K., and Shaked, Y. (2020). The multifaceted role of mesenchymal stem cells in cancer. Semin. Cancer Biol. *60*, 225–237.
21. Fan, S., Gao, H., Ji, W., Zhu, F., Sun, L., Liu, Y., Zhang, S., Xu, Y., Yan, Y., and Gao, Y. (2020). Umbilical cord-derived mesenchymal stromal/stem cells expressing IL-24 induce apoptosis in gliomas. J. Cell Physiol. *235*, 1769–1779.
22. Chulpanova, D.S., Kitaeva, K.V., Tazetdinova, L.G., James, V., Rizvanov, A.A., and Solovyeva, V.V. (2018). Application of mesenchymal stem cells for therapeutic agent delivery in anti-tumor treatment. Front. Pharmacol. *9*, 259.
23. Bitsika, V., Roubelakis, M.G., Zagoura, D., Trohatou, O., Makridakis, M., Pappa, K.I., Marini, F.C., Vlahou, A., and Anagnou, N.P. (2012). Human amniotic fluid-derived mesenchymal stem cells as therapeutic vehicles: a novel approach for the treatment of bladder cancer. Stem Cells Dev. *21*, 1097–1111.
24. Lazennec, G., and Jorgensen, C. (2008). Concise review: adult multipotent stromal cells and cancer: risk or benefit? Stem Cells *26*, 1387–1394.
25. Cortes-Dericks, L., and Galetta, D. (2019). The therapeutic potential of mesenchymal stem cells in lung cancer: benefits, risks and challenges. Cell Oncol. (Dordr) *42*, 727–738.
26. Poh, A. (2016). First oncolytic viral therapy for melanoma. Cancer Discov. *6*, 6.
27. Greig, S.L. (2016). Talimogene laherparepvec: first global approval. Drugs *76*, 147–154.
28. Yang, Y., Xu, W., Peng, D., Wang, H., Zhang, X., Wang, H., Xiao, F., Zhu, Y., Ji, Y., Gulukota, K., et al. (2019). An oncolytic adenovirus targeting transforming growth factor β inhibits protumorigenic signals and produces immune activation: a novel approach to enhance anti-PD-1 and anti-CTLA-4 therapy. Hum. Gene Ther. *30*, 1117–1132.
29. Liu, Z., Yang, Y., Zhang, X., Wang, H., Xu, W., Wang, H., Xiao, F., Bai, Z., Yao, H., Ma, X., et al. (2017). An oncolytic adenovirus encoding decorin and granulocyte macrophage colony stimulating factor inhibits tumor growth in a colorectal tumor model by targeting pro-tumorigenic signals and via immune activation. Hum. Gene Ther. *28*, 667–680.
30. Small, E.J., Carducci, M.A., Burke, J.M., Rodriguez, R., Fong, L., van Ummersen, L., Yu, D.C., Aimi, J., Ando, D., Working, P., et al. (2006). A phase I trial of intravenous CG7870, a replication-selective, prostate-specific antigen-targeted oncolytic adenovirus, for the treatment of hormone-refractory, metastatic prostate cancer. Mol. Ther. *14*, 107–117.
31. Hamid, O., Varterasian, M.L., Wadler, S., Hecht, J.R., Benson, A., 3rd., Galanis, E., Uprichard, M., Omer, C., Bycott, P., Hackman, R.C., et al. (2003). Phase II trial of intravenous CI-1042 in patients with metastatic colorectal cancer. J. Clin. Oncol. *21*, 1498–1504.
32. Ahi, Y.S., Bangari, D.S., and Mittal, S.K. (2011). Adenoviral vector immunity: its implications and circumvention strategies. Curr. Gene Ther. *11*, 307–320.
33. Xu, W., Zhang, Z., Yang, Y., Hu, Z., Wang, C.H., Morgan, M., Wu, Y., Hutten, R., Xiao, X., Stock, S., et al. (2014). Ad5/48 hexon oncolytic virus expressing sTGFβRIIFc produces reduced hepatic and systemic toxicities and inhibits prostate cancer bone metastases. Mol. Ther. *22*, 1504–1517.
34. Coughlan, L., Bradshaw, A.C., Parker, A.L., Robinson, H., White, K., Custers, J., Goudsmit, J., Van Roijen, N., Barouch, D.H., Nicklin, S.A., et al. (2012). Ad5:Ad48 hexon hypervariable region substitutions lead to toxicity and increased inflammatory responses following intravenous delivery. Mol. Ther. *20*, 2268–2281.
35. Alba, R., Bradshaw, A.C., Parker, A.L., Bhella, D., Waddington, S.N., Nicklin, S.A., van Rooijen, N., Custers, J., Goudsmit, J., Barouch, D.H., et al. (2009). Identification of coagulation factor (F)X binding sites on the adenovirus serotype 5 hexon: effect of mutagenesis on FX interactions and gene transfer. Blood *114*, 965–971.
36. Li, Z., Fan, D., and Xiong, D. (2015). Mesenchymal stem cells as delivery vectors for anti-tumor therapy. Stem Cell Investig. *2*, 6.
37. Khakoo, A.Y., Pati, S., Anderson, S.A., Reid, W., Elshal, M.F., Rovira, ., II, Nguyen, A.T., Malide, D., Combs, C.A., Hall, G., et al. (2006). Human mesenchymal stem cells exert potent antitumorigenic effects in a model of Kaposi's sarcoma. J. Exp. Med. *203*, 1235–1247.
38. Ahn, J.O., Coh, Y.R., Lee, H.W., Shin, I.S., Kang, S.K., and Youn, H.Y. (2015). Human adipose tissue-derived mesenchymal stem cells inhibit melanoma growth in vitro and in vivo. Anticancer Res. *35*, 159–168.
39. Yoon, A.R., Hong, J., Li, Y., Shin, H.C., Lee, H., Kim, H.S., and Yun, C.O. (2019). Mesenchymal stem cell-mediated delivery of an oncolytic adenovirus enhances antitumor efficacy in hepatocellular carcinoma. Cancer Res. *79*, 4503–4514.
40. Du, W., Seah, I., Bougazzoul, O., Choi, G., Meeth, K., Bosenberg, M.W., Wakimoto, H., Fisher, D., and Shah, K. (2017). Stem cell-released oncolytic herpes simplex virus has therapeutic efficacy in brain metastatic melanomas. Proc. Natl. Acad. Sci. U S A *114*, E6157–E6165.
41. Ahmed, A.U., Tyler, M.A., Thaci, B., Alexiades, N.G., Han, Y., Ulasov, I.V., and Lesniak, M.S. (2011). A comparative study of neural and mesenchymal stem cell-based carriers for oncolytic adenovirus in a model of malignant glioma. Mol. Pharm. *8*, 1559–1572.
42. Liu, Y., Ren, H., Zhou, Y., Shang, L., Zhang, Y., Yang, F., and Shi, X. (2019). The hypoxia conditioned mesenchymal stem cells promote hepatocellular carcinoma progression through YAP mediated lipogenesis reprogramming. J. Exp. Clin. Cancer Res. *38*, 228.
43. Nishikawa, G., Kawada, K., Nakagawa, J., Toda, K., Ogawa, R., Inamoto, S., Mizuno, R., Itatani, Y., and Sakai, Y. (2019). Bone marrow-derived mesenchymal stem cells promote colorectal cancer progression via CCR5. Cell Death Dis. *10*, 264.
44. Yamaguchi, Y., Mann, D.M., and Ruoslahti, E. (1990). Negative regulation of transforming growth factor-beta by the proteoglycan decorin. Nature *346*, 281–284.
45. Flavell, R.A., Sanjabi, S., Wrzesinski, S.H., and Licona-Limón, P. (2010). The polarization of immune cells in the tumour environment by TGFbeta. Nat. Rev. Immunol. *10*, 554–567.
46. Marcoe, J.P., Lim, J.R., Schaubert, K.L., Fodil-Cornu, N., Matka, M., McCubbrey, A.L., Farr, A.R., Vidal, S.M., and Laouar, Y. (2012). TGF-β is responsible for NK cell immaturity during ontogeny and increased susceptibility to infection during mouse infancy. Nat. Immunol. *13*, 843–850.
47. Liu, S., Chen, S., and Zeng, J. (2018). TGF-β signaling: a complex role in tumorigenesis (Review). Mol. Med. Rep. *17*, 699–704.
48. Jazowiecka-Rakus, J., Sochanik, A., Rusin, A., Hadryś, A., Fidyk, W., Villa, N., Rahman, M.M., Chmielik, E., Franco, L.S., and McFadden, G. (2020). Myxoma virus-loaded mesenchymal stem cells in experimental oncolytic therapy of murine pulmonary melanoma. Mol. Ther. Oncol. *18*, 335–350.
49. Lu, L.L., Liu, Y.J., Yang, S.G., Zhao, Q.J., Wang, X., Gong, W., Han, Z.B., Xu, Z.S., Lu, Y.X., Liu, D., et al. (2006). Isolation and characterization of human umbilical cord mesenchymal stem cells with hematopoiesis-supportive function and other potentials. Haematologica *91*, 1017–1026.